8-1-2024

Cholesterol accumulation promotes photoreceptor senescence and retinal degeneration

Ryo Terao
Washington University School of Medicine in St. Louis
Brian S Sohn
Washington University School of Medicine in St. Louis
Taku Yamamoto
Washington University School of Medicine in St. Louis
Tae Jun Lee
Washington University School of Medicine in St. Louis
Jason Colasanti
Washington University School of Medicine in St. Louis

See next page for additional authors

Cholesterol Accumulation Promotes Photoreceptor Senescence and Retinal Degeneration

Ryo Terao,[1,2] Brian S. Sohn,[1] Taku Yamamoto,[1,3] Tae Jun Lee,[1] Jason Colasanti,[1] Charles W. Pfeifer,[1] Joseph B. Lin,[1] Andrea Santeford,[1] Shinobu Yamaguchi,[1] Mitsukuni Yoshida,[1,4] and Rajendra S. Apte[1,5,6]

[1]John F. Hardesty, MD, Department of Ophthalmology & Visual Sciences, Washington University School of Medicine, St. Louis, Missouri, United States
[2]Department of Ophthalmology, Graduate School of Medicine, the University of Tokyo, Tokyo, Japan
[3]Department of Ophthalmology, Faculty of Medicine and Graduate School of Medicine, Hokkaido University, Hokkaido, Japan
[4]Department of Anesthesiology, Washington University School of Medicine, St. Louis, Missouri, United States
[5]Department of Medicine, Washington University School of Medicine, St. Louis, Missouri, United States
[6]Department of Developmental Biology, Washington University School of Medicine, St. Louis, Missouri, United States

Correspondence: Rajendra S. Apte, 660 South Euclid Avenue, Box 8096-06-0705, St. Louis, MO 63110, USA;
apte@wustl.edu.
Mitsukuni Yoshida, 660 South Euclid Avenue, Box 8096-06-0705, St. Louis, MO 63110, USA;
mitsukuni@wustl.edu.

MY and RSA contributed equally to the work presented here.

Received: April 28, 2024
Accepted: August 1, 2024
Published: August 21, 2024

Citation: Terao R, Sohn BS, Yamamoto T, et al. Cholesterol accumulation promotes photoreceptor senescence and retinal degeneration. *Invest Ophthalmol Vis Sci.* 2024;65(10):29. https://doi.org/10.1167/iovs.65.10.29

Purpose. Dysregulated cholesterol metabolism is critical in the pathogenesis of AMD. Cellular senescence contributes to the development of numerous age-associated diseases. In this study, we investigated the link between cholesterol burden and the cellular senescence of photoreceptors.

Methods. Retinas from rod-specific ATP binding cassette subfamily A member 1 (*Abca1*) and G member 1 (*Abcg1*) (*Abca1/g1*$^{-rod/-rod}$) knockout mice fed with a high-fat diet were analyzed for the signs of cellular senescence. Real-time quantitative PCR and immunofluorescence were used to characterize the senescence profile of the retina and cholesterol-treated photoreceptor cell line (661W). Inducible elimination of p16(Ink4a)-positive senescent cells (INK-ATTAC) mice or the administration of senolytic drugs (dasatinib and quercetin: D&Q) were used to examine the impact of senolytics on AMD-like phenotypes in *Abca1/g1*$^{-rod/-rod}$ retina.

Results. Increased accumulation of senescent cells as measured by markers of cellular senescence was found in *Abca1/g1*$^{-rod/-rod}$ retina. Exogenous cholesterol also induced cellular senescence in 661W cells. Selective elimination of senescent cells in *Abca1/g1*$^{-rod/-rod}$;INK-ATTAC mice or by administration of D&Q improved visual function, lipid accumulation in retinal pigment epithelium, and Bruch's membrane thickening.

Conclusions. Cholesterol accumulation promotes cellular senescence in photoreceptors. Eliminating senescent photoreceptors improves visual function in a model of retinal neurodegeneration, and senotherapy offers a novel therapeutic avenue for further investigation.

Keywords: age-related macular degeneration, cholesterol, ATP binding cassette transporter A1, cellular senescence, senolytics, neurodegeneration, photoreceptor

Cholesterol is a sterol lipid essential for cellular and systemic functions to maintain mammalian homeostasis.[1] As a major component of the plasma membrane, cholesterol maintains its integrity and fluidity.[2] However, the excess accumulation of intracellular cholesterol with age induces membrane fluidity disruption, cytokine production, and endoplasmic reticulum (ER) stress, eventually leading to an inflammatory state and cell death.[3–5] Therefore disrupted cholesterol metabolism leads to age-related diseases, including neurodegenerative eye diseases and cardiovascular diseases.[6–8]

AMD is a leading cause of blindness in the elderly population in industrialized countries.[9] In early stages, patients present with lipid-rich deposits in subretinal- or sub-retinal pigment epithelium (RPE) spaces (i.e., subretinal drusenoid deposits or drusen), which contain lipids including cholesterol in abundance.[10,11] Genome-wide association studies have found that polymorphisms in genes involved in lipid metabolism such as apolipoprotein E, cholesteryl ester transfer protein, and ATP binding cassette (ABC) subfamily A member 1 (ABCA1) are associated with increased AMD risk. [12–14] Abca1 is a transmembrane transporter necessary for the cellular efflux of cholesterol and phospholipids.[15] cholesterol efflux pathway is essential to maintain appropriate intracellular cholesterol levels by transporting it out of cells.[16] We previously demonstrated that the deficiency

of *Abca1* and *Abcg1* in photoreceptors leads to photoreceptor degeneration and lipid accumulation in RPE.[17] However, how dysregulated cholesterol metabolism in photoreceptors drives the pathogenesis of retinal degeneration needs further elucidation.

Cellular senescence, a state of cell cycle arrest in response to various stressors such as DNA damage and organelle stress as well as general aging, has emerged as an important contributor to age-related diseases.[18,19] Senescent cells are characterized by increased expression of $p16^{Ink4a}$ and $p21^{CIP1/WAF1}$ (coded by *Cdkn2a* and *Cdkn1a*, respectively), senescence-associated β-galactosidase (SA-β-Gal) activity, and secretion of senescence-associated secretory phenotypes (SASP) such as vascular endothelial growth factor and tumor necrosis factor-alpha (TNF-α). Furthermore, through SASP, senescent cells propagate cellular senescence in neighboring tissues and promote sterile chronic inflammation.[20] Senotherapy by genetic and pharmacological removal of senescent cells (senolytics) ameliorates age-related phenotypes and neurodegenerative diseases.[21,22] In addition to the cellular senescence of proliferating cells, there are several reports of cellular senescence of terminally differentiated and nonproliferating cells including astrocytes, microglia, and macrophages.[23,24] Recent reports have found that age-related neurodegenerative diseases such as Alzheimer's disease are associated with cellular senescence.[25] Our recent study also demonstrated that cholesterol accumulation within the retina increases with age and that senescent macrophages deficient in *Abca1/g1* contribute to the development of neurodegeneration and subretinal lipid-rich deposits in mice,[26] indicating a potential role for increased cholesterol burden in promoting cellular senescence in retinal diseases. A series of studies by Crespo-Garcia and colleagues[27] demonstrated the crucial role of cellular senescence in ocular diseases. Senescent cells accumulate in the retina of patients with proliferative diabetic retinopathy and in the mouse model of oxygen-induced retinopathy. Cells associated with vascular units were enriched in senescence-related transcripts. Clearance of senescent cells in a genetic model and small molecular inhibitor of anti-apoptotic protein BCL-xL suppressed pathological angiogenesis.[27] A recent study revealed that neutrophil-mediated clearance of senescent vascular endothelial cells promoted the remodeling of unhealthy vessels, further highlighting the potential importance of these processes in AMD pathogenesis.[28] Phase I clinical trial on UBX1325 (foselutoclax), a senolytic small-molecule inhibitor of BCL-xL, demonstrated safety in patients with diabetic retinopathy and is currently undergoing a phase 2 efficacy study.[29]

We hypothesized that the dysregulated cholesterol metabolism in photoreceptors induced their cellular senescence and promoted the accumulation of subretinal lipid and retinal degeneration, thereby displaying some features of AMD. Because esterified and unesterified cholesterol contained in the outer segments of photoreceptors are potential sources of lipid accumulation in RPE cells and drusen in human AMD,[10,30] we investigated whether cholesterol accumulation in photoreceptors in the rod-specific *Abca1/Abcg1* knockout mouse model promotes cellular senescence in the retina. We also examined the potential utility of senolytics against the development of AMD-like phenotypes to find a possible therapeutic opportunity to target age-related retinal dysfunction and photoreceptor degeneration secondary to lipid accumulation.

Material and Methods

Mice

All animal experiments were conducted in accordance with the ARVO Statement for the Use of Animals in Ophthalmic and Vision Research and Washington University School of Medicine in St. Louis Animal Care and Use guidelines and after approval by the Institutional Animal Care and Use Committee. All mice in this study were housed in a 12-hour light/dark cycle with free access to food and water. To generate mice deficient in *Abca1* and *Abcg1* in photoreceptors (*Abca1/g1*$^{-rod/-rod}$), *Abca1*$^{flox/flox}$/*Abcg1*$^{flox/flox}$ (*Abca1/g1*$^{f/f}$) mice purchased from the Jackson Laboratory (021067) were crossed with mice with Rhodopsin-iCre75 transgene mice, which were originally provided by Dr. Ching-Kang Jason Chen.[31,32] INK-ATTAC transgene mice were provided by Unity Biotechnology[33] and crossed with *Abca1/g1*$^{-rod/-rod}$ to generate *Abca1/g1*$^{-rod/-rod}$;INK-ATTAC. All mice used for experiments in this study were fed a high-fat diet (HFD; 60% fat) from six weeks of age for six weeks. In individual experimental groups of mice, littermates of the same sex were used.

Cells

The photoreceptor cell line (661W) was provided by Dr. Muayyad Al Ubaidi and maintained as previously described.[31,34,35] Cells were plated and cultured in a humidified incubator at 37°C with 5% carbon dioxide with Dulbecco's modified Eagle medium containing 10% fetal bovine serum and 1% penicillin-streptomycin (Gibco, 15140-122; Thermo Fisher Scientific, Waltham, MA, USA). The following day, cells were serum-starved overnight. A cholesterol solution with methyl-β-cyclodextrin (C4951; Sigma-Aldrich Corp., St. Louis, MO, USA) was added to each well and incubated for 24 hours.

Drug Treatments

To ablate $p16^{Ink4a}$-positive senescent cells, *Abca1/g1*$^{-rod/-rod}$;INK-ATTAC mice were treated with an intraperitoneal injection of AP20187 (B1274, 10 mg/kg BW; Apexbio Technology LLC, Houston, TX, USA) every other day while on HFD. AP20187 reconstituted in ethanol (50 mg/ml) was diluted by polyethylene glycol (PEG) 400, tween 80, and H_2O. For pharmacological senolysis, mice were treated with the combination of dasatinib (SML2589, 5 mg/kg BW; Sigma-Aldrich Corp.) and quercetin (Q4951, 50 mg/kg BW; Sigma-Aldrich Corp.) dissolved in dimethyl sulfoxide, tween 20, PEG 400, and H_2O. The vehicle was used for controls. Dasatinib and quercetin (D+Q) were administrated on weekdays every two weeks via oral gavage during the HFD feeding.

RNA Isolation and Quantitative Polymerase Chain Reaction (qPCR)

Samples were collected in TRIzol reagent to isolate RNA. Dissected retina and RPE/choroid samples from mice were homogenized before RNA isolation. According to the manufacturer's instructions, mRNA was obtained using NucleoSpin RNA columns (740955; Takara Biotechnology Co., Kyoto, Japan). DNase (D4527; Sigma-Aldrich) diluted with DNA digestion buffer (E1010-1; Zymo Research, Irvine,

Table. QPCR Probes

Gene	Taqman Gene Reference
β-actin	Mm02619580_g1
Cdkn1a (*p21*^{CIP1})	Mm04205640_g1
Cdkn2a (*p16*^{Ink4a})	Mm00494449_m1
Tnf-α	Mm00443258_m1
Abc1a	Mm01350770_m1
Abcg1	Mm01348250_m1
Cxcl12	Mm00445553_m1
Ccl2	Mm00441242_m1

CA, USA) was used for gDNA removal. CDNA was generated using a cDNA reverse transcription kit (4368813; Applied Biosystems, Foster City, CA, USA). The probes used in this study are shown in the Table. QPCR was performed using probes for each target gene and TaqMan Fast Advanced Master Mix (4444554; Applied Biosystems). TaqMan array standard plates were purchased from Thermo Fisher Scientific (4391524) and customized to evaluate the senescence markers identified in a previous study.[36] β-actin was used as the internal control. MRNA transcript levels were measured using StepOnePlus Real-Time PCR System (Thermo Fisher Scientific). Relative expression of target genes normalized to β-actin was calculated using the ΔΔCt method.

Fluorescence In Situ Hybridization (FISH)

Fresh frozen sagittal section and cultured cells were used for FISH. Samples were fixed with 10% formalin, dehydrated, and incubated with protease reagents (322381; Advanced Cell Diagnostics, Newark, CA, USA). Probes against *Cdkn1a and Cdkn2a* (408551 and 411011; Advanced Cell Diagnostics), also known as *p21*$^{CIP1/WAF1}$ and *p16*^{Ink4a}, respectively, were added on each slide and incubated at 40°C for two hours in a HybEZ Oven (241000ACD; Advanced Cell Diagnostics). Amplification and color development were performed using RNAscope 2.5 HD detection reagents (322360; Advanced Cell Diagnostics) according to the manufacturer's instructions. Nuclei were stained with DAPI (5 µg/mL). Images were taken using the LSM 800 with a 20 × 0.80 N.A. Plan-Apochromat objective and processed with ZEN Microscopy Software.

Immunofluorescence

Slides were fixed with 10% formalin for 15 minutes. PBS containing 5% BSA and 0.1% Triton X-100 was used for blocking and permeabilization. Slides were incubated with anti-Iba-1 (NB100-1028; Novus Biologicals, Littleton, CO, USA), anti-P2RY12 (AS-55043A; Anaspec, Fremont, CA, USA), anti-GFAP (13-0300; Thermo Fisher Scientific), and anti-Ki67(ab15580; Abcam, Cambridge, MA, USA) as primary antibodies overnight at 4°C. The next day, slides were incubated with Alexa Fluor-conjugated corresponding secondary antibodies at room temperature for 1 hour. DAPI solution (5 µg/ml) was used for nuclear staining. Images were taken using a Zeiss LSM 800 microscope (Zeiss, Oberkochen, Germany) with 20 × 0.80 N.A. Plan-Apochromat, 63 × 1.40 Plan-Apochromat, and 100 × 1.45 alpha Plan-Fluor objectives. Images were processed with ZEN Microscopy Software.

Electroretinography

Mice were dark-adapted overnight. The following day, mice were anesthetized by intraperitoneal injection of 122 mg/kg ketamine and 14.1 mg/kg xylazine. Both eyes were treated topically with 1% tropicamide to dilate pupils. After anesthesia, mice were placed on a heating pad to maintain body temperature at 37°C. The ground and reference needle electrodes were placed in the base of the tail and the skin between the eyes, respectively. Contact lens electrodes were placed on the corneas bilaterally. ERG was performed using UTAS BigShot System (LKC Technologies Inc., Gaithersburg, MD, USA) under dark red-light illumination. A sequence of white light flash (10 µs) with stepwise intensity was used as full-field flash stimuli. The amplitude of a-wave was calculated as the difference from the baseline to the lowest point soon after the stimuli. The amplitude of b-wave was calculated as the difference between the trough of the a-wave and the peak of the b-wave as previously described.[17,37,38]

Transmission Electron Microscopy

For ultrastructural analyses, the anterior segment, including the cornea, ciliary body, and lens in enucleated eyeballs, were removed. Eyecups were fixed in 2% paraformaldehyde/2.5% glutaraldehyde (Ted Pella Inc., Redding, CA, USA) in 0.1 M sodium cacodylate buffer for two hours at room temperature and then overnight at 4°C. Samples were washed in sodium cacodylate buffer and post-fixed in 1% osmium tetroxide (Ted Pella Inc.) for one hour at room temperature. Samples were washed three times in distilled water, followed by en bloc staining in 1% aqueous uranyl acetate (Electron Microscopy Sciences, Hatfield, PA, USA) for 1 hour. Samples were then rinsed in distilled water, dehydrated in a graded series of ethanol, and embedded in Eponate 12 resin (Ted Pella Inc). Sectioning was performed using a Leica Ultracut UCT ultramicrotome (Leica Microsystems, Bannockburn, IL, USA) at 95 nm. Sections were stained with uranyl acetate and lead citrate and viewed on a JEOL 1200 EX transmission electron microscope (JEOL USA Inc., Peabody, MA, USA) equipped with an AMT 8 megapixel digital camera and AMT Image Capture Engine V602 software (Advanced Microscopy Techniques, Woburn, MA, USA). EM images were randomly taken from multiple fields of the retina by an EM core. The number of intracellular lipids in the retinal pigment epithelium and Bruch's membrane thickness in each sample were evaluated by calculating the average of multiple EM images.

Lipid Measurements

Liver, adipose, and plasma samples were collected from indicated mice. Mice were fasted for 6 hours to avoid the potential effects of feeding on lipid profiles. Tissue samples were collected in a 2 mL homogenizer tube pre-loaded with 2.8 mm ceramic beads (no. 19-628; Omni International, Kennesaw, GA, USA), while plasma samples were collected in Eppendorf tubes.

PBS 0.75 mL was added to the tube and homogenized in the Omni Bead Ruptor Elite (three cycles of 10 seconds at 5 m/s with a 10-second dwell time). Homogenate containing 2 to 6 mg of original tissue was transferred to a glass tube for extraction. A modified Bligh and Dyer extraction was carried out on all samples.[39] Prior to biphasic extraction, an internal standard mixture consisting of 70

lipid standards across 17 subclasses was added to each sample (5040156 [AB Sciex, Toronto, Canada], Avanti 330827 [Avanti Polar Lipids, Inc., Alabaster, AL, USA], Avanti 330830 [Avanti Polar Lipids, Inc.], Avanti 330828 [Avanti Polar Lipids, Inc.], Avanti 791642 [Avanti Polar Lipids, Inc.]). After two successive extractions, pooled organic layers were dried down in a SpeedVac SPD300DDA (Thermo Fisher Scientific) using ramp setting 4 at 35° for 45 minutes with a total run time of 90 minutes. Lipid samples were resuspended in 1:1 methanol/dichloromethane with 10 mM Ammonium Acetate and transferred to robovials (10800107; Thermo Fisher Scientific,) for analysis. Samples were analyzed on the Sciex 5500 with a DMS device (Lipidyzer Platform; SCIEX, Framingham, MA, USA) with an expanded targeted acquisition list of 1450 lipid species across 17 subclasses. Quantitative values were normalized to mg of tissue.

Statistical Analysis

Statistical analysis was performed using GraphPad Prism. A two-tailed, unpaired student's *t*-test was used to compare the two groups. A one-way ANOVA with the Bonferroni post-hoc test was used to compare three or more means. Two-way ANOVA followed by Bonferroni correction was performed for comparison with multiple time points. Statistically significant outliers were excluded from the analysis. $P < 0.05$ was considered statistically significant. Data were presented as bar or line graphs (mean ± standard error of the mean). When indicated, dot plots show each value.

Results

Dysregulated Cholesterol Metabolism in the Retina Drives Photoreceptor Senescence

Our previous study demonstrated that *Abca1/g1*$^{-rod/-rod}$ mice fed with HFD for six weeks present with lipid accumulation in RPE cells and photoreceptor neurodegeneration, mimicking some features of AMD.[17] In addition, diet-induced obesity has been shown to induce neuroinflammation and retinal neurodegeneration in models of AMD.[40] Given that cellular senescence is an emerging contributor to the pathogenesis of AMD, we sought to detect senescent cells in the eyes of *Abca1/g1*$^{-rod/-rod}$.

p16 and p21 are cyclin-dependent kinase inhibitors that regulate cell cycle arrest and are expressed at the initiation of cellular senescence.[41] qPCR revealed that the expression of *p16* and *p21* was significantly increased in retinas isolated from *Abca1/g1*$^{-rod/-rod}$ compared to control (*Abca1/g1*$^{f/f}$). The expression of *Tnf-α* in the RPE-choroid complex significantly increased in *Abca1/g1*$^{-rod/-rod}$ (Fig. 1A). FISH identified increased numbers of *p16* and *p21*-positive cells in the outer nuclear layer (ONL) of *Abca1/g1*$^{-rod/-rod}$ (Fig. 1B). Of note, while some *p21*-positive cells were also observed in the inner layer (INL) of both the control and *Abca1/g1*$^{-rod/-rod}$ retinas, there was no difference in the prevalence of p21-positive cells in INL between the two groups. These results suggest impaired cholesterol efflux in rod photoreceptors promotes cellular senescence in the ONL.

The ONL of the retina contains the nuclei of photoreceptors. However, during diverse pathological conditions that drive photoreceptor degeneration, immune cells such as microglia and monocyte-derived macrophages exit the plexiform layers and migrate into the ONL or INL.[42–44] To examine whether the senescent cells detected in ONL of *Abca1/g1*$^{-rod/-rod}$ mice are immune cells, we performed immunofluorescent staining for astrocytes, Müller glial cells, microglia, and macrophages. GFAP-positive astrocytes and Müller glial cells, Iba-1-positive microglia and macrophages, and P2RY12-positive microglia were rarely observed in ONL (Fig. 1C). Moreover, there were no differences in the distribution of immune cells between *Abca1/g1*$^{-rod/-rod}$ and control retina, suggesting that immune cells did not infiltrate into the ONL in *Abca1/g1*$^{-rod/-rod}$ (Fig. 1D). These data demonstrate that deficiency of cholesterol efflux cell-autonomously promotes cellular senescence of photoreceptors but does not induce senescence of neighboring immune cells and glial cells.

Cholesterol Accumulation Promotes Photoreceptor Senescence

Based on the histological analysis of *Abca1/g1*$^{-rod/-rod}$ retina showing that the majority of senescent cells in *Abca1/g1*$^{-rod/-rod}$ were photoreceptors, we evaluated the impact of cholesterol burden on senescence profiles of photoreceptor cells in vitro using the 661W immortalized murine photoreceptor cell line. Exogenous cholesterol treatment promoted the expression of *Abca1* and *Abcg1*, demonstrating that the 50 µM concentration was sufficient to promote the expression of cholesterol homeostatic response in photoreceptors (Fig. 2A). Increasing concentration of cholesterol promoted the expression of *p16* and *p21* in a dose-dependent manner (Fig. 2B). Consistently, upregulation of these senescence markers was validated by FISH (Fig. 2C). Moreover, the expression of previously reported SASP factors secreted by photoreceptors, including tumor necrosis factor *Tnf-α* and *Cxcl12*, were upregulated by cholesterol treatment in 661W (Fig. 2D). We further quantified the expression of other previously reported senescence markers.[36] Senescence markers such as *Ccnd1*, *Dda1*, *Fam214b*, *Gdnf*, *Plk3*, *Slc19a2*, and *Tollip* were upregulated (Fig. 2E). Given that a hallmark of cellular senescence includes terminal cell-cycle arrest, we quantified the levels of Ki67, a marker of cell proliferation. While photoreceptors are terminally differentiated cells, Ki67 is commonly used to characterize the senescence status in a photoreceptor cell line.[45] Cholesterol treatment substantially decreased the expression of Ki67 in 661W cells (Figs. 2F, 2G). These results support that cholesterol upregulates the expressions of SASP and senescence markers and induces cell-cycle arrest in photoreceptor cells, thereby inducing their cellular senescence.

Senescence Clearance in a Genetic Model Suppresses Retinal Neurodegeneration

To evaluate the effects of senolytics on senescence clearance and retinal dysfunction in *Abca1/g1*$^{-rod/-rod}$ mice, we used INK-ATTAC mice to selectively eliminate senescent cells. INK-ATTAC is a transgenic mouse expressing FKBP-caspase 8 fusion protein under the *p16*^{INK4a} promoter. The administration of AP20187, a cell-permeable ligand used to dimerize FKBP fusion proteins, can ablate p16^{Ink4a} -positive senescent cells in INK-ATTAC mice through the activation of FKBP-fused caspase 8.[33,46] We generated *Abca1/g1*$^{-rod/-rod}$; INK-ATTAC mice and examined the efficacy of senescence clearance and effects on retinal function and retinal degeneration in *Abca1/g1*$^{-rod/-rod}$ mice (Fig. 3A).

Investigative Ophthalmology & Visual Science

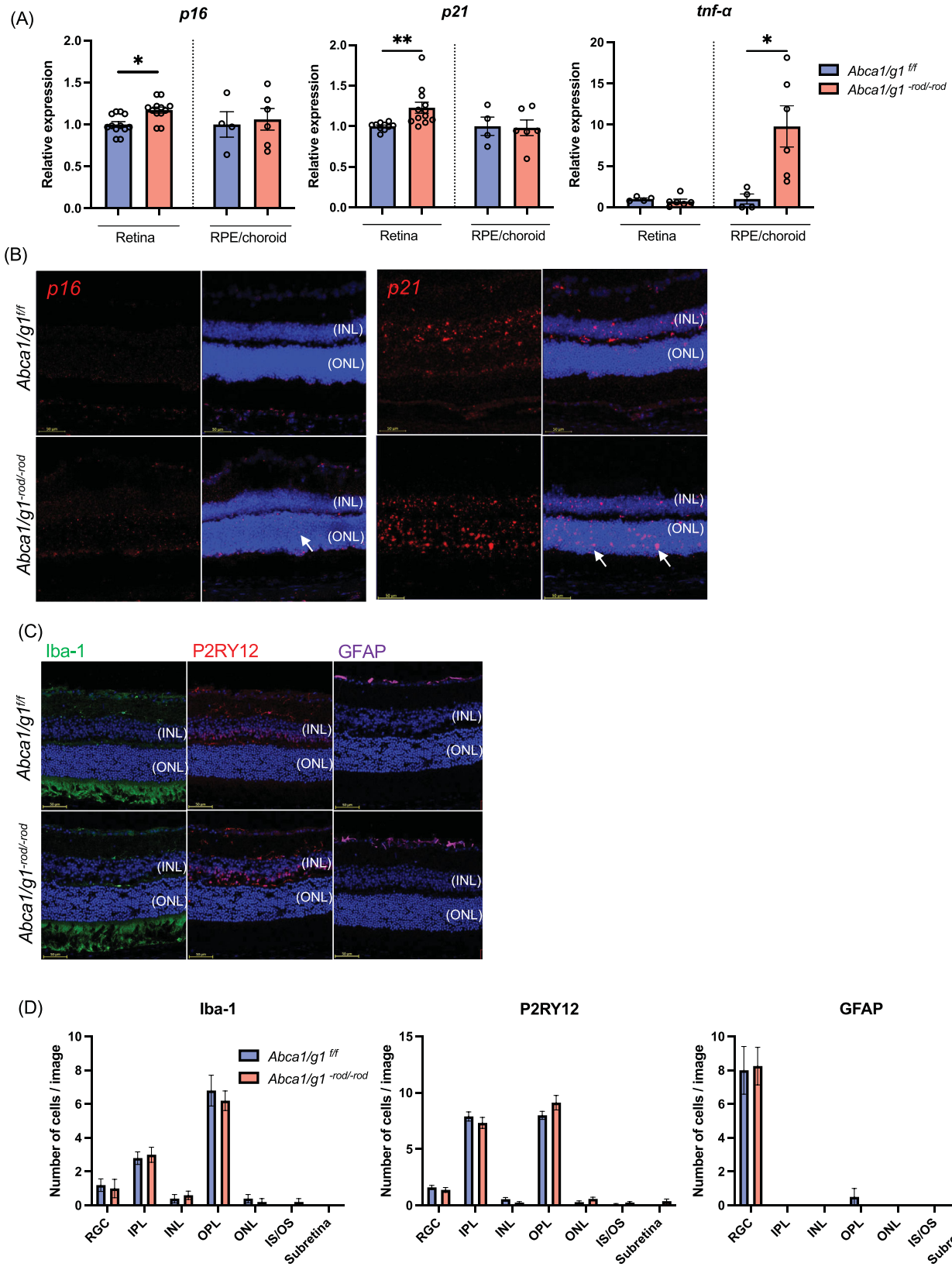

Figure 1. Cholesterol accumulation in the retina promotes photoreceptor senescence. (**A**) mRNA expression of senescence markers (*p16* and *p21*) and *Tnf-α* in the retina and RPE/choroid complex isolated from *Abca1/g1*$^{f/f}$ and *Abca1/g1*$^{-rod/-rod}$ fed by the high-fat diet. (**B**) Images of FISH (*p16* and *p21*) (*red*) of retinal sections. Arrows indicate positive cells in the outer nuclear layer. (**C**) Immunofluorescence images of retinal sections stained for Iba-1, P2RY12, and GFAP. Nuclei were stained with DAPI (*blue*). (**D**) The quantification of Iba-1-, P2RY12-, and GFAP-positive cells in each retinal layer. *$P < 0.05$; **$P < 0.01$, *t*-test for comparison between two groups, one-way ANOVA followed by Bonferroni correction for multiple comparisons. Data are represented as mean ± SEM.

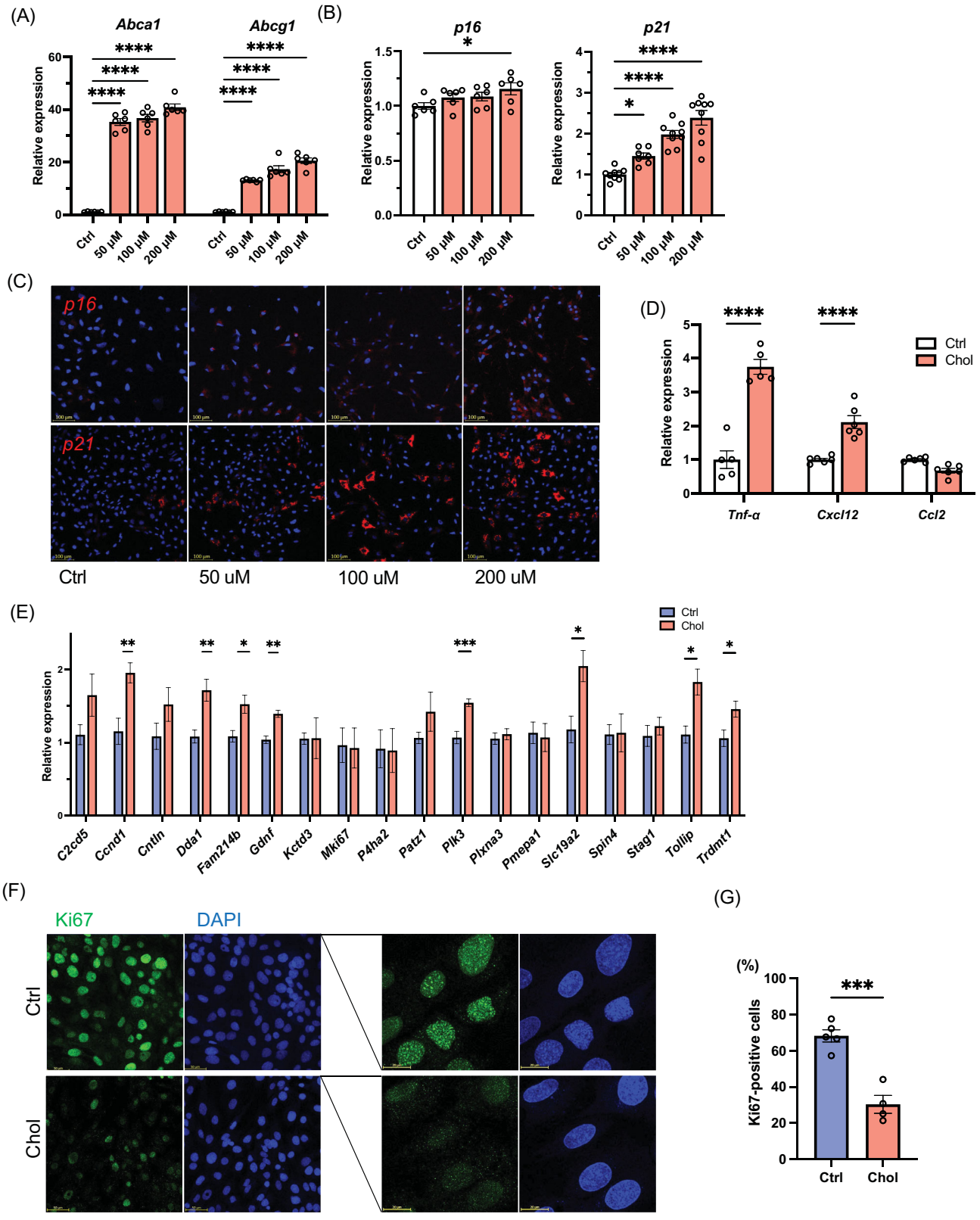

Figure 2. Characterization of cellular senescence in photoreceptor cells treated with cholesterol in vitro. mRNA expression of *Abca1*, *Abcg1* (**A**), and senescence markers (*p16* and *p21*) (**B**) in photoreceptor cell line 661W treated with cholesterol for 24 hours. (**C**) ISH (*p16* and *p21*) (*red*) of photoreceptor cell line treated with cholesterol. (**D**) mRNA expression of inflammatory cytokines (*Tnf-α*, *Cxcl12b*, and *Ccl2*) in a photoreceptor cell line treated with cholesterol. (**E**) qPCR senescence array. (**F**) Immunofluorescence of photoreceptor cell line stained for Ki67 (*green*). Nuclei were stained with DAPI (*blue*). (**G**) The quantification of Ki67-positive cells. *$P < 0.05$; **$P < 0.01$, ***$P < 0.001$, ****$P < 0.0001$, *t*-test for comparison between two groups, one-way ANOVA followed by Bonferroni correction for multiple comparisons.

Investigative Ophthalmology & Visual Science

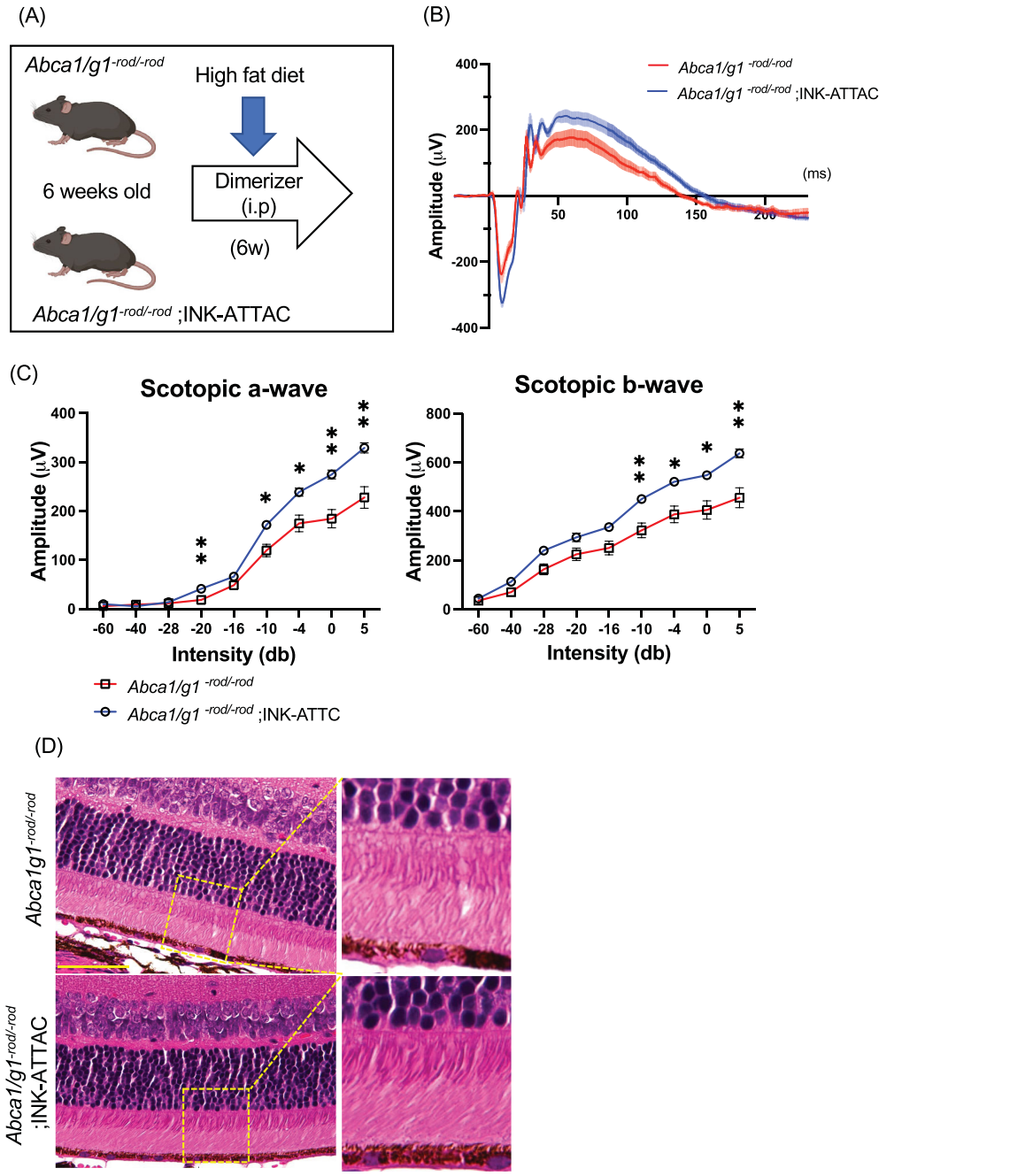

Figure 3. Selective elimination of p16-positive senescent cells suppresses retinal dysfunction and degeneration in rod-specific cholesterol efflux-deficient mice. (**A**) Experimental design using *Abca1/g1*$^{-rod/-rod}$;INK-ATTAC. (**B**) Electroretinography waveform of *Abca1/g1*$^{-rod/-rod}$ and *Abca1/g1*$^{-rod/-rod}$;INK-ATTAC. Each waveform and graph indicate the mean ± SEM. (**C**) The quantification of ERG (scotopic a-wave and b-wave) amplitudes. (**D**) Images of H&E staining. *Scale bar*: 50 μm. **P* < 0.05; ***P* < 0.01, two-way ANOVA followed by Bonferroni correction. Data are represented as mean ± SEM.

INK-ATTAC significantly improved the retinal function quantified by scotopic a- and b-waves as detected by electroretinography (ERG), suggesting that the clearance of senescent cells improves visual function in *Abca1/g1*$^{-rod/-rod}$ mice (Figs. 3B, 3C). Histological images showed that senescence clearance caused no adverse morphological changes (Fig. 3D). Structural analysis using electron microscopy (EM) found that the number of lipid droplets in RPE cells was significantly reduced in *Abca1/g1*$^{-rod/-rod}$;INK-ATTAC mice (Figs. 4A, 4B). Thickening of Bruch's membrane at the basal boundary of RPE occurs with age and in patients with AMD. and was seen as previously reported in reduced *Abca1/g1*$^{-rod/-rod}$ mice on a high-fat diet.[47,48] Thickening of Bruch's membrane was also significantly reduced *Abca1/g1*$^{-rod/-rod}$;INK-ATTAC mice (Figs. 4A, 4C). Consistently, INK-ATTAC suppressed the expression of *p21* in the retina and both *p21* and *Tnf-α* in the RPE/choroid, suggesting that senescence clearance ameliorated the senescent state in the retina seen with cholesterol accumulation (Fig. 4D). Body fat percentage, cholesterol levels in plasma

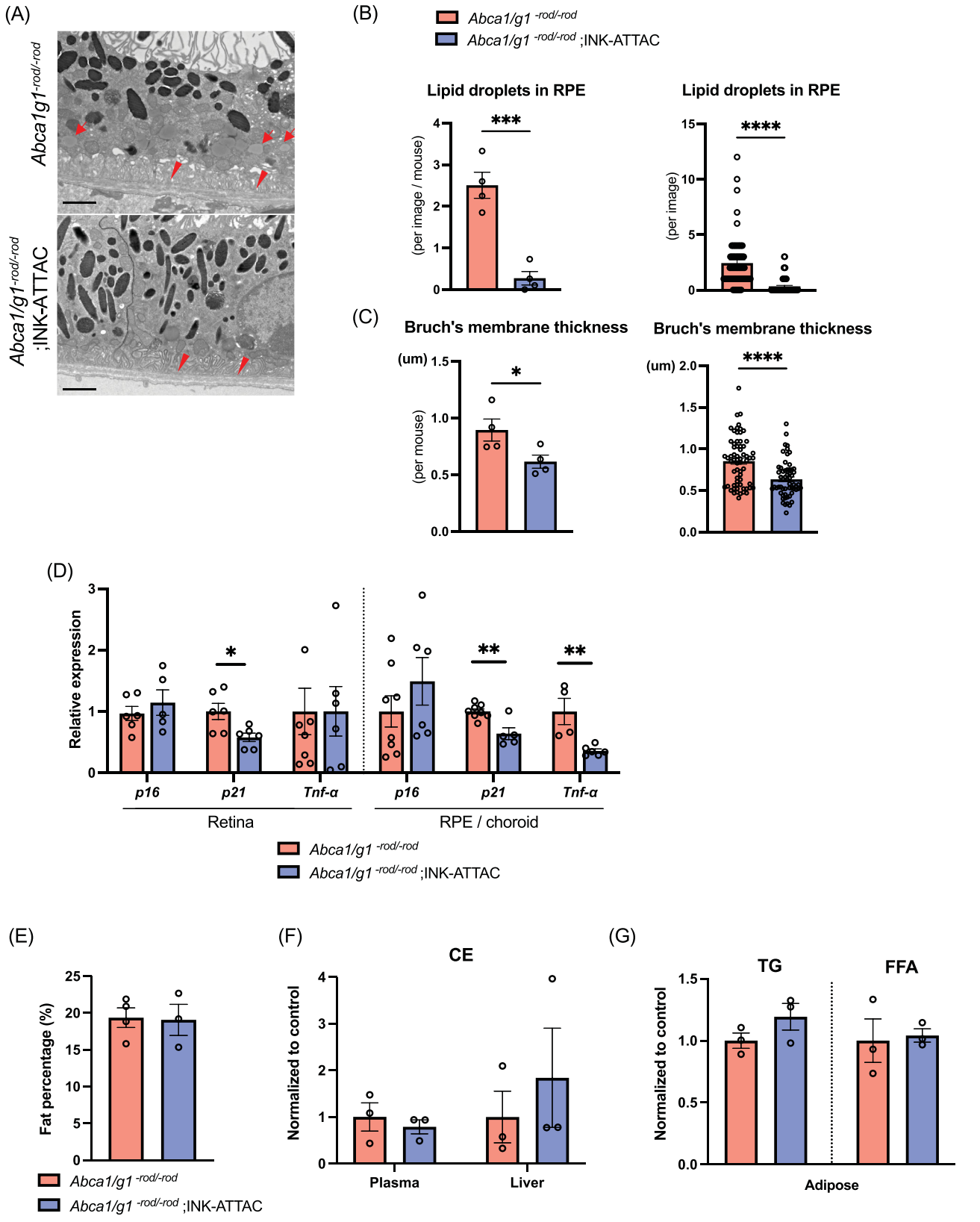

Figure 4. Selective elimination of p16-positive senescent cells suppresses AMD-associated phenotype and senescence without altering systemic lipid metabolism. Representative electron microscopy images showing RPE cells and Bruch's membrane (**A**), and the quantification of the number of intracellular lipids in RPE cells (**B**) and Bruch's membrane thickness (**C**). *Scale bar*: 2 µm. Note intracellular lipids in RPE cells (*arrow*) and thickened Bruch's membrane (*arrowhead*) in *Abca1/g1*$^{-rod/-rod}$. (**D**) mRNA expression of senescence markers (*p16* and *p21*) and *Tnf-α* in the retina and RPE/choroid complex isolated from *Abca1/g1*$^{-rod/-rod}$ and *Abca1/g1*$^{-rod/-rod}$;INK-ATTAC. Fat percentage (**E**), cholesterol ester in plasma and liver (F), and triglyceride and free fatty acids in adipose tissue (**G**) of *Abca1/g1*$^{-rod/-rod}$ and *Abca1/g1*$^{-rod/-rod}$;INK-ATTAC. $^{*}P < 0.05$; $^{**}P < 0.01$; $^{***}P < 0.001$; $^{****}P < 0.0001$, *t*-test. Data are represented as mean ± SEM.

Investigative Ophthalmology & Visual Science

and liver, and triglycerides and free fatty acids in adipose tissue were not improved in *Abca1/g1*$^{-rod/-rod}$;INK-ATTAC mice (Figs. 4E–G). These findings suggest that senescence clearance did not ameliorate systemic metabolic dysregulation, such as hypercholesteremia, but had a targeted effect on the retinal structure and function. These results indicate that senolytics can prevent retinal neurodegeneration and lipid accumulation in RPE induced by cholesterol efflux deficit in photoreceptors without altering systemic metabolic dysregulation.

Pharmacological Senolysis Improves Retinal Neurodegeneration

D+Q are two of the most studied senolytic drugs that reduce the senescence burden, extend lifespan, and improve age-related functional decline in mice.[49] To examine if pharmacological senolytics can alter retinal phenotypes, we treated *Abca1/g1*$^{-rod/-rod}$ mice with D+Q (Fig. 5A). Similar to senolysis by INK-ATTAC, D+Q treatment by oral gavage significantly improved retinal function quantified by the amplitude of a- and b-waves measured by ERG (Figs. 5B, 5C). There were no noticeable morphological changes in histology (Fig. 5D). Morphological changes, including intracellular lipid accumulation in RPE and Bruch's membrane thickening, were significantly suppressed by D+Q (Figs. 5E–G). Like the results in INK-ATTAC, D+Q did not improve body fat percentage (Fig. 5H). These results indicate that D+Q mitigates retinal dysfunction induced in HFD-treated Abca1/g1-rod/-rod.

Discussion

In these studies, we evaluated cellular senescence in the retina induced by the accumulation of cholesterol in photoreceptors. Recent studies suggest a close relationship between cholesterol metabolism and cellular senescence.[50] A previous report showed that cholesterol induces the senescence of vascular smooth muscle cells through ER stress and mitochondrial reactive oxygen species.[51] Moreover, 7-ketocholesterol induces pancreatic β-cell senescence, presumably through SIRT1/CDK4–Rb–E2F1 pathway.[52] Our group previously demonstrated that cholesterol accumulation caused by impaired efflux secondary to *Abca1/Abcg1* deficiency combined with increased influx from HFD promoted macrophage senescence that led to features of retinal neurodegeneration and subretinal lipid-rich deposits in a murine AMD model.[26] In this previous study, depletion of nicotinamide adenine dinucleotide by liver X receptor/CD38 was responsible for cholesterol-induced macrophage senescence and mitochondrial dysfunction. Another report revealed that T cells deficient in *Abca1/Abcg1* developed senescence.[53] As a therapeutic approach, a cholesterol-lowering drug, probucol, has been shown to have suppressive effects against senescence in human mesangial cells.[54] Although the underlying mechanism varies depending on the cell type, these studies suggest that the cholesterol influx and efflux imbalance drives cellular senescence in diverse cell types.

Although cellular senescence was originally defined as cell cycle arrest of proliferating cells, terminally differentiated post-mitotic neuronal cells can also develop senescence that leads to cellular dysfunction and a proinflammatory state that ultimately contributes to age-related neurodegeneration.[55,56] Senescent neurons are characterized by the increase in levels of p21, γH2AX, and SASP factors such as IL-6, NF-$\kappa\beta$, IL-β, and CXCL1.[56,57] Here we show that specialized neurons such as photoreceptors can also develop senescence as a consequence of cholesterol overload secondary to impaired cholesterol efflux. Senescence states of photoreceptors were characterized by an increase in senescence markers, including p16, p21, γH2AX, SA-β-Gal, and SASP factors (TNF-α and Cxcl12), and a decrease in Ki67.[45,58] Senescent cells secrete proinflammatory molecules triggering inflammation in neighboring tissues and systemically in a paracrine or endocrine manner.[59] SASP factors ultimately drive an age-related sterile inflammatory state known as inflammaging.[60] In senescent photoreceptors, proinflammatory cytokines such as TNF-α, MCP-1, IL-6, and Cxcl12 are upregulated, highlighting their potential role in influencing parainflammation within their micromilieu.[58] In this study, while senescence markers were upregulated in photoreceptors, RPE did not exhibit senescent profiles except for an SASP factor, TNF-α. TNF-α plays a pivotal role in regulating the immune response and is involved in the pathogenesis of AMD.[61,62] Our current study found that RPE in our murine models and 661W cells treated with cholesterol showed increased expression of TNF-α. These results indicate that cholesterol accumulation drives an inflammatory response in diverse cell types in the retina.

We further investigated the effects of senolysis in a murine AMD model by using a genetic model and senolytic drugs. Because senolytics did not improve the systemic metabolic derangement by HFD, we concluded that the therapeutic effects of senolytics in *Abca1/g1*$^{-rod/-rod}$ are derived from the clearance of local senescent cells in the eye. Senolytics are an emerging therapeutic approach against diverse neurodegenerative diseases.[63] INK-ATTAC suppresses the tau-dependent neurodegenerative disease and preserves cognitive function by removing senescent cells in the hippocampus and cortex.[23] Senolytics can reduce neuronal loss and cognitive decline in Alzheimer's disease models through the elimination of senescent neurons.[21,64,65] These reports suggest that the clearance of senescent neurons could be beneficial for treating age-related neurodegenerative diseases. Although the removal of senescent neurons may have a deleterious effect on neuronal function and worsen the underlying neurodegeneration, our data revealed retinal functional recovery by senolytics. Therefore our study suggests that the protective effects on nonsenescent photoreceptors outweigh the adverse effects of the clearance of senescent photoreceptors on retinal function.

There are several limitations to this study. First, 661W is a photoreceptor cell line generated by the expression of SV40 T antigen.[35] SV40-LT immortalizes cells by inactivating p53/Rb,[66] which can further suppress p21 as the downstream target and prevent cellular senescence under baseline culture conditions. Therefore suppressed p21 activity due to the immortalization process may alter the cellular behavior of photoreceptor cells and their physiological response to cholesterol burden. Second, although some features of AMD are observed in *Abca1/g1*$^{-rod/-rod}$ mice, it is likely that cellular senescence of multiple cell types is involved in the AMD process, thereby limiting the mechanistic insight into human AMD. However, in conjunction with our study revealing the interaction of dysregulated cholesterol metabolism, myeloid cell senescence, and AMD, the study supports the importance of cholesterol burden on the senescence phenotype across a wide range of cell types.[8,26,58] Because impaired

Investigative Ophthalmology & Visual Science

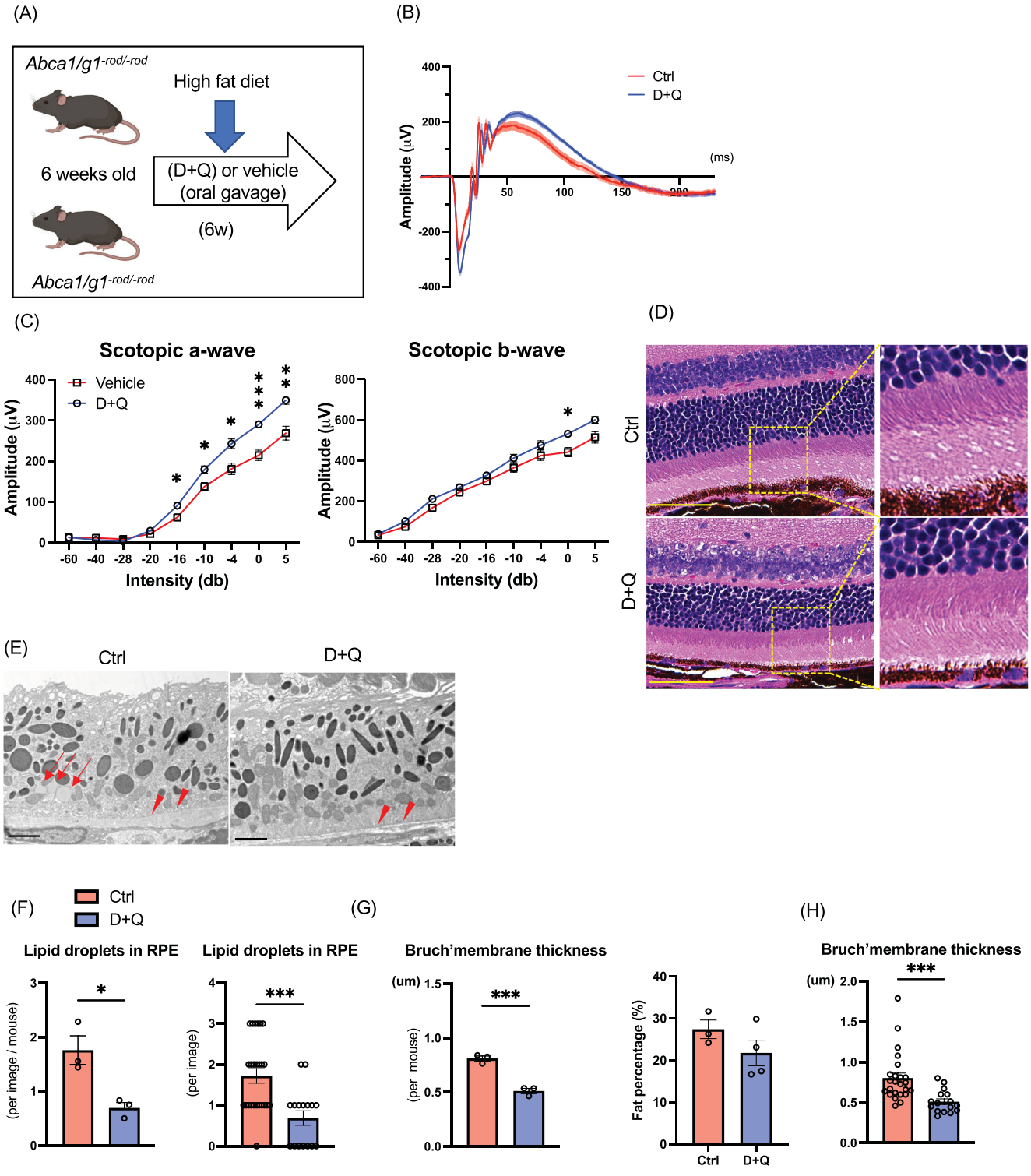

Figure 5. Effects of pharmacological senolysis on retinal degeneration by cholesterol accumulation in photoreceptors. (**A**) Experimental design of senolytic drug administration (D+Q) for *Abca1/g1*$^{-rod/-rod}$. (**B**) Electroretinography (ERG) waveform of *Abca1/g1*$^{-rod/-rod}$ treated with D+Q or vehicle. (**C**) The quantification of ERG (scotopic a-wave and b-wave) amplitudes. (**D**) Images of H&E staining. *Scale bar*: 50 µm. Representative electron microscopy images showing (**E**) RPE cells and Bruch's membrane, (**F**) the quantification of the number of intracellular lipids in RPE cells, and (**G**) Bruch's membrane thickness. *Scale bar*: 2 µm. Note that intracellular lipids in RPE cells (*arrow*) and thickened Bruch's membrane (*arrowhead*) in *Abca1/g1*$^{-rod/-rod}$ were treated with the vehicle. (**H**) Fat percentages of *Abca1/g1*$^{-rod/-rod}$ treated with D+Q. **P* < 0.05; ***P* < 0.01; ****P* < 0.001, *t*-test for comparison between two groups and two-way ANOVA followed by Bonferroni correction for comparison with multiple time points. Data are represented as mean ± SEM.

Investigative Ophthalmology & Visual Science

cholesterol efflux in RPE also mimics early-stage AMD,[67] we will investigate the biological relationship between dysregulated cholesterol metabolism and cellular senescence in RPE cells in future studies.

In summary, these studies revealed that photoreceptor senescence induced by cholesterol is responsible for visual dysfunction in a murine model of AMD and provided a mechanical insight into cholesterol-induced photoreceptor dysfunction. They also support the therapeutic potential of senolytics against AMD.

Acknowledgments

The authors thank Wandy L. Beatty, Molecular Microbiology Imaging Facility in Washington University School of Medicine, for electron microscopy analysis and the University of California Los Angeles lipidomics lab for the lipid measurement service.

Supported by National Institutes of Health (NIH) grant P30 EY02687 (Vision Core Grant); Jeffrey T. Fort Innovation Fund (RSA); Starr Foundation AMD Research Fund (RSA); Siteman Retina Research Fund (RSA); Carl Marshall and Mildred Almen Reeves Foundation (RSA); Retina Associates of St. Louis Research Fund (RSA); an unrestricted grant from Research to Prevent blindness to the John F. Hardesty, MD Department of Ophthalmology and Visual Sciences at Washington University School of Medicine in St. Louis; Williams D. Owens Anesthesiology Research Fellowship Award (M.Y.); McDonnell Center for Systems Neuroscience Small Grants Program (M.Y.); Bayer Retina Award in Japan (RT); the International Retinal Research Foundation (RT); Japan Society for the Promotion of Science Overseas Research Fellowship (RT), KAKENHI Grant JP24K23505 (RT). TL was supported by NIH Training Grant (1T32GM1397740-1). CWP was supported by the Washington University in St. Louis Vision Science Training grant (T32 EY013360), Vitreoretinal Surgery Foundation Fellowship (VGR0023118), and McDonnell Center for Cellular and Molecular Neurobiology Small Grants Program (GF0011083). JBL was supported by the NIH grant (F30DK130282) and the Washington University in St. Louis Medical Scientist Training Program (NIH grant T32GM07200).

Disclosure: **R. Terao**, None; **B.S. Sohn**, None; **T. Yamamoto**, None; **T.J. Lee**, None; **J. Colasanti**, None; **C.W. Pfeifer**, None; **J.B. Lin**, None; **A. Santeford**, None; **S. Yamaguchi**, None; **M. Yoshida**, Institute for Research on Productive Aging (P); **R.S. Apte**, Roche (C), New Amsterdam Pharma (C), QBio (C), Delavie Sciences (C), Liberty Biosecurity (C), Metro Biotech (O), Mobius Scientific (O), Washington University (P)

References

1. Morgan AE, Mooney KM, Wilkinson SJ, Pickles NA, Mc Auley MT. Cholesterol metabolism: a review of how ageing disrupts the biological mechanisms responsible for its regulation. *Ageing Res Rev*. 2016;27:108–124.
2. Rone MB, Fan J, Papadopoulos V. Cholesterol transport in steroid biosynthesis: role of protein-protein interactions and implications in disease states. *Biochim Biophys Acta*. 2009;1791:646–658.
3. Sene A, Apte RS. Eyeballing cholesterol efflux and macrophage function in disease pathogenesis. *Trends Endocrinol Metab*. 2014;25:107–114.
4. Wang N, Westerterp M. ABC transporters, cholesterol efflux, and implications for cardiovascular diseases. *Adv Exp Med Biol*. 2020;1276:67–83.
5. Zahid MDK, Rogowski M, Ponce C, Choudhury M, Moustaid-Moussa N, Rahman SM. CCAAT/enhancer-binding protein beta (C/EBPbeta) knockdown reduces inflammation, ER stress, and apoptosis, and promotes autophagy in oxLDL-treated RAW264.7 macrophage cells. *Mol Cell Biochem*. 2020;463:211–223.
6. Martins IJ, Hone E, Foster JK, et al. Apolipoprotein E, cholesterol metabolism, diabetes, and the convergence of risk factors for Alzheimer's disease and cardiovascular disease. *Mol Psychiatry*. 2006;11:721–736.
7. Cheung CMG, Gan A, Fan Q, et al. Plasma lipoprotein subfraction concentrations are associated with lipid metabolism and age-related macular degeneration. *J Lipid Res*. 2017;58:1785–1796.
8. Sene A, Khan AA, Cox D, et al. Impaired cholesterol efflux in senescent macrophages promotes age-related macular degeneration. *Cell Metab*. 2013;17:549–561.
9. Apte RS. Age-Related Macular Degeneration. *N Engl J Med*. 2021;385:539–547.
10. Curcio CA. Soft drusen in age-related macular degeneration: biology and targeting via the oil spill strategies. *Invest Ophthalmol Vis Sci*. 2018;59:AMD160–AMD181.
11. Wang L, Clark ME, Crossman DK, et al. Abundant lipid and protein components of drusen. *PLoS One*. 2010;5:e10329.
12. Neale BM, Fagerness J, Reynolds R, et al. Genome-wide association study of advanced age-related macular degeneration identifies a role of the hepatic lipase gene (LIPC). *Proc Natl Acad Sci USA*. 2010;107:7395–7400.
13. Chen W, Stambolian D, Edwards AO, et al. Genetic variants near TIMP3 and high-density lipoprotein-associated loci influence susceptibility to age-related macular degeneration. *Proc Natl Acad Sci USA*. 2010;107:7401–7406.
14. Winkler TW, Grassmann F, Brandl C, et al. Genome-wide association meta-analysis for early age-related macular degeneration highlights novel loci and insights for advanced disease. *BMC Med Genomics*. 2020;13:120.
15. Qian H, Zhao X, Cao P, Lei J, Yan N, Gong X. Structure of the human lipid exporter ABCA1. *Cell*. 2017;169:1228–1239.e1210.
16. He P, Gelissen IC, Ammit AJ. Regulation of ATP binding cassette transporter A1 (ABCA1) expression: cholesterol-dependent and - independent signaling pathways with relevance to inflammatory lung disease. *Respir Res*. 2020;21:250.
17. Ban N, Lee TJ, Sene A, et al. Disrupted cholesterol metabolism promotes age-related photoreceptor neurodegeneration. *J Lipid Res*. 2018;59:1414–1423.
18. Di Micco R, Krizhanovsky V, Baker D, d'Adda di Fagagna F. Cellular senescence in ageing: from mechanisms to therapeutic opportunities. *Nat Rev Mol Cell Biol*. 2021;22:75–95.
19. Childs BG, Durik M, Baker DJ, van Deursen JM. Cellular senescence in aging and age-related disease: from mechanisms to therapy. *Nat Med*. 2015;21:1424–1435.
20. Coppe JP, Patil CK, Rodier F, et al. Senescence-associated secretory phenotypes reveal cell-nonautonomous functions of oncogenic RAS and the p53 tumor suppressor. *PLoS Biol*. 2008;6:2853–2868.
21. Zhang P, Kishimoto Y, Grammatikakis I, et al. Senolytic therapy alleviates Abeta-associated oligodendrocyte progenitor cell senescence and cognitive deficits in an Alzheimer's disease model. *Nat Neurosci*. 2019;22:719–728.
22. Wang Y, Tseng Y, Chen K, et al. Dasatinib plus quercetin alleviates choroid neovascularization by reducing the cellular senescence burden in the RPE-choroid. *Invest Ophthalmol Vis Sci*. 2023;64:39.
23. Bussian TJ, Aziz A, Meyer CF, Swenson BL, van Deursen JM, Baker DJ. Clearance of senescent glial cells prevents tau-dependent pathology and cognitive decline. *Nature*. 2018;562:578–582.

Investigative Ophthalmology & Visual Science

24. Englund DA, Jolliffe A, Aversa Z, et al. p21 induces a senescence program and skeletal muscle dysfunction. *Mol Metab*. 2023;67:101652.
25. Wang Q, Duan L, Li X, et al. Glucose metabolism, neural cell senescence and Alzheimer's disease. *Int J Mol Sci*. 2022;23:4351.
26. Terao R, Lee TJ, Colasanti J, et al. LXR/CD38 activation drives cholesterol-induced macrophage senescence and neurodegeneration via NAD(+) depletion. *Cell Rep*. 2024;43(5):114102.
27. Crespo-Garcia S, Tsuruda PR, Dejda A, et al. Pathological angiogenesis in retinopathy engages cellular senescence and is amenable to therapeutic elimination via BCL-xL inhibition. *Cell Metab*. 2021;33:818–832.e817.
28. Binet F, Cagnone G, Crespo-Garcia S, et al. Neutrophil extracellular traps target senescent vasculature for tissue remodeling in retinopathy. *Science*. 2020;369(6506):eaay5356.
29. Crespo-Garcia S, Fournier F, Diaz-Marin R, et al. Therapeutic targeting of cellular senescence in diabetic macular edema: preclinical and phase 1 trial results. *Nat Med*. 2024;30:443–454.
30. Curcio CA, Presley JB, Malek G, Medeiros NE, Avery DV, Kruth HS. Esterified and unesterified cholesterol in drusen and basal deposits of eyes with age-related maculopathy. *Exp Eye Res*. 2005;81:731–741.
31. Lin JB, Kubota S, Ban N, et al. NAMPT-Mediated NAD(+) Biosynthesis Is Essential for Vision In Mice. *Cell Rep*. 2016;17:69–85.
32. Li S, Chen D, Sauve Y, McCandless J, Chen YJ, Chen CK. Rhodopsin-iCre transgenic mouse line for Cre-mediated rod-specific gene targeting. *Genesis*. 2005;41:73–80.
33. Baker DJ, Childs BG, Durik M, et al. Naturally occurring p16(Ink4a)-positive cells shorten healthy lifespan. *Nature*. 2016;530:184–189.
34. Tan E, Ding XQ, Saadi A, Agarwal N, Naash MI, MR Al-Ubaidi. Expression of cone-photoreceptor-specific antigens in a cell line derived from retinal tumors in transgenic mice. *Invest Ophthalmol Vis Sci*. 2004;45:764–768.
35. al-Ubaidi MR, Font RL, Quiambao AB, et al. Bilateral retinal and brain tumors in transgenic mice expressing simian virus 40 large T antigen under control of the human interphotoreceptor retinoid-binding protein promoter. *J Cell Biol*. 1992;119:1681–1687.
36. Hernandez-Segura A, de Jong TV, Melov S, Guryev V, Campisi J, Demaria M. Unmasking Transcriptional Heterogeneity in Senescent Cells. *Curr Biol*. 2017;27:2652–2660.e2654.
37. Lee TJ, Sasaki Y, Ruzycki PA, et al. Catalytic isoforms of AMP-activated protein kinase differentially regulate IMPDH activity and photoreceptor neuron function. *JCI Insight*. 2024;9(4).
38. Ban N, Lee TJ, Sene A, et al. Impaired monocyte cholesterol clearance initiates age-related retinal degeneration and vision loss. *JCI Insight*. 2018;3(17).
39. Hsieh WY, Williams KJ, Su B, Bensinger SJ. Profiling of mouse macrophage lipidome using direct infusion shotgun mass spectrometry. *STAR Protoc*. 2021;2:100235.
40. Hata M, Andriessen E, Hata M, et al. Past history of obesity triggers persistent epigenetic changes in innate immunity and exacerbates neuroinflammation. *Science*. 2023;379:45–62.
41. Huang W, Hickson LJ, Eirin A, Kirkland JL, Lerman LO. Cellular senescence: the good, the bad and the unknown. *Nat Rev Nephrol*. 2022;18:611–627.
42. Zeiss CJ, Johnson EA. Proliferation of microglia, but not photoreceptors, in the outer nuclear layer of the rd-1 mouse. *Invest Ophthalmol Vis Sci*. 2004;45:971–976.
43. O'Koren EG, Yu C, Klingeborn M, et al. Microglial Function Is Distinct in Different Anatomical Locations during Retinal Homeostasis and Degeneration. *Immunity*. 2019;50:723–737.e727.
44. Pfeifer CW, Walsh JT, Santeford A, et al. Dysregulated CD200-CD200R signaling in early diabetes modulates microglia-mediated retinopathy. *Proc Natl Acad Sci USA*. 2023;120:e2308214120.
45. Liang J, Yao F, Fang D, et al. Hyperoside alleviates photoreceptor degeneration by preventing cell senescence through AMPK-ULK1 signaling. *FASEB J*. 2023;37:e23250.
46. Baker DJ, Wijshake T, Tchkonia T, et al. Clearance of p16Ink4a-positive senescent cells delays ageing-associated disorders. *Nature*. 2011;479:232–236.
47. Okubo A, Rosa RH, Jr., Bunce CV, et al. The relationships of age changes in retinal pigment epithelium and Bruch's membrane. *Invest Ophthalmol Vis Sci*. 1999;40:443–449.
48. Karampelas M, Sim DA, Keane PA, et al. Evaluation of retinal pigment epithelium-Bruch's membrane complex thickness in dry age-related macular degeneration using optical coherence tomography. *Br J Ophthalmol*. 2013;97:1256–1261.
49. Xu M, Pirtskhalava T, Farr JN, et al. Senolytics improve physical function and increase lifespan in old age. *Nat Med*. 2018;24:1246–1256.
50. Roh K, Noh J, Kim Y, et al. Lysosomal control of senescence and inflammation through cholesterol partitioning. *Nat Metab*. 2023;5:398–413.
51. Wang L, Wang M, Niu H, et al. Cholesterol-induced HRD1 reduction accelerates vascular smooth muscle cell senescence via stimulation of endoplasmic reticulum stress-induced reactive oxygen species. *J Mol Cell Cardiol*. 2024;187:51–64.
52. Zhu Q, Wang W, Wu N, et al. 7-Ketocholesterol accelerates pancreatic beta-cell senescence by inhibiting the SIRT1/CDK4-Rb-E2F1 signaling pathway. *Islets*. 2023;15:2219105.
53. Bazioti V, La Rose AM, Maassen S, et al. T cell cholesterol efflux suppresses apoptosis and senescence and increases atherosclerosis in middle aged mice. *Nat Commun*. 2022;13:3799.
54. Zhou H, Huang B, Han Y, Jin R, Chen S. Probucol inhibits JAK2-STAT pathway activation and protects human glomerular mesangial cells from tert-butyl hydroperoxide induced premature senescence. *Can J Physiol Pharmacol*. 2013;91:671–679.
55. Wong GC, Chow KH. DNA Damage Response-Associated Cell Cycle Re-Entry and Neuronal Senescence in Brain Aging and Alzheimer's Disease. *J Alzheimers Dis*. 2023;94:S429–S451.
56. von Zglinicki T, Wan T, Miwa S. Senescence in post-mitotic cells: a driver of aging? *Antioxid Redox Signal*. 2021;34:308–323.
57. Jurk D, Wang C, Miwa S, et al. Postmitotic neurons develop a p21-dependent senescence-like phenotype driven by a DNA damage response. *Aging Cell*. 2012;11:996–1004.
58. Lee KS, Lin S, Copland DA, Dick AD, Liu J. Cellular senescence in the aging retina and developments of senotherapies for age-related macular degeneration. *J Neuroinflammation*. 2021;18:32.
59. Krtolica A, Campisi J. Cancer and aging: a model for the cancer promoting effects of the aging stroma. *Int J Biochem Cell Biol*. 2002;34:1401–1414.
60. Khavinson V, Linkova N, Dyatlova A, Kantemirova R, Kozlov K. Senescence-associated secretory phenotype of cardiovascular system cells and inflammaging: perspectives of peptide regulation. *Cells*. 2022;12.
61. Wan L, Lin HJ, Tsai Y, et al. Tumor necrosis factor-alpha gene polymorphisms in age-related macular degeneration. *Retina*. 2010;30:1595–1600.

Investigative Ophthalmology & Visual Science

62. Papadopoulos Z. The role of the cytokine TNF-alpha in choroidal neovascularization: a systematic review. *Eye (Lond)*. 2024;38:25–32.
63. Melo Dos Santos LS, Trombetta-Lima M, Eggen B, Demaria M. Cellular senescence in brain aging and neurodegeneration. *Ageing Res Rev*. 2024;93:102141.
64. Musi N, Valentine JM, Sickora KR, et al. Tau protein aggregation is associated with cellular senescence in the brain. *Aging Cell*. 2018;17:e12840.
65. Herdy JR, Traxler L, Agarwal RK, et al. Increased post-mitotic senescence in aged human neurons is a pathological feature of Alzheimer's disease. *Cell Stem Cell*. 2022;29:1637–1652.e1636.
66. Umehara K, Sun Y, Hiura S, et al. A new conditionally immortalized human fetal brain pericyte cell line: establishment and functional characterization as a promising tool for human brain pericyte studies. *Mol Neurobiol*. 2018;55:5993–6006.
67. Storti F, Klee K, Todorova V, et al. Impaired ABCA1/ABCG1-mediated lipid efflux in the mouse retinal pigment epithelium (RPE) leads to retinal degeneration. *Elife*. 2019;8:e45100.

Investigative Ophthalmology & Visual Science